



A novel crosslinked amphoteric adsorbent thiourea formaldehyde calcium alginate: preparation, characterization and adsorption behaviors of removing color from acidic and basic dyes

Ashraf A. El-Bindary*, Hala A. Kiwaan, Abdel Ghany F. Shoair, Ahmed R. Hawas

Chemistry Department, Faculty of Science, University of Damietta, Damietta34517, Egypt,
emails: abindary@yahoo.com (A.A. El-Bindary), hkiwaan@gmail.com (H.A. Kiwaan),
abdel_shoair@yahoo.com (A.F. Shoair), ahmed_hawas_a_h@yahoo.com (A.R. Hawas)

Received 9 July 2018; Accepted 20 January 2019

ABSTRACT

Thiourea formaldehyde alginate resin (TUFA) was prepared and characterized performed by Fourier transform infrared spectrometer (FT-IR) spectra, scanning electron microscope (SEM)/EDS, Energy dispersive X-ray analysis (EDX) and X-ray diffraction (XRD). The amphoteric grafting resin used for removal of both anionic Congo red (CR) and cationic crystal violet (CV) dyes individual from aqueous solutions by batch adsorption method. The adsorption–desorption behaviors of TUFA resin were investigated under various pH values, initial CR and CV concentrations, contact time, solution temperatures, adsorbent dose and ionic strength were examined by batch technique. The highest sorption capacities of CR and CV after 90 min at 25°C were found at pH of 5 and 9, respectively. The equilibrium data were analyzed by the isothermal adsorption models and the applicability of empirical kinetic models was also studied. The maximum monolayer coverage (q_m) from Langmuir isotherm model was determined to be 559.55 and 237.77 mg.g⁻¹ for CR and CV respectively. The kinetic adsorption behavior gives the best agreement to pseudo-second order model of the experimental data. Thermodynamic parameters including ΔG° , ΔS° and ΔH° were determined over the temperature range of 293–318 K. The results revealed that adsorption reaction of both dyes was spontaneous endothermic and physical in nature.

Keywords: Amphoteric resin; Color removal; Isotherm; Kinetics; Congo red; Crystal violet

1. Introduction

Water pollution is one of the most serious environmental problems and control of it is the major thrust areas of scientific research [1]. That duo to colored organic compounds generally imparts only a minor fraction of the organic load to wastewaters. The direct discharge of this wastewater into environment affects its ecological status by causing various undesirable changes [2]. Water scarcity and strict legislation make water reuse in dye related industries like textile and leather become more important. Textile industry is one of the most chemically intensive industries on the earth and the major

polluter of water. It generates huge quantities of complex chemical substances as a part of unused materials including dyes in the form of wastewater during various stages of textile processing. During chemical industrial processing about 2% of produced dyes are continuously entering the water systems due to improper processing and dyeing methods from these industries [3]. The dyes are difficult to decolorize due to their complex structure and most of the dyes contain aromatic rings, which make them mutagenic and carcinogenic that effects on aquatic organisms and human health. Most of the used dyes are synthetic dyes which grouped into acidic, basic, direct, reactive and azodyes [4]. However, color removal

* Corresponding author.

from textile wastewater by means of cheaper and environmentally friendly technologies is still a major challenge. Among various methods including biological treatments, physio-chemical and physical processes have been tested for the treatment of dye containing effluents [5]. Biological processes are the most cost-effective ones for wastewater treatment but didn't always appear relevant for dye removal for the low or total absence of biodegradability of this class of pollutants. Physio-chemical processes, such as oxidation or advanced oxidation processes are efficient but costly due to the high required energy. Physical techniques such as adsorption, chemical precipitation (coagulation-flocculation–electroflocculation), ion exchange and membrane separation (ultrafiltration - reverse osmosis) can also be efficiently used to remove these recalcitrant pollutants [6]. Among physical processes, adsorption technique is considered to be one the most effective and certain technology due to its simplicity (easy handling), high efficiency and economic feasibility as well as the availability of a wide ranges of adsorbents that potential and competitive method for treatment of dyes wastewater treatment [7]. Various kinds of materials including cationic and anionic resin have been found to be capable of removing various dyes pollutants from wastewater [8]. In this study, CR and CV were selected as dyes to be removed from its aqueous solution using thiourea formaldehyde alginate resin (TUFA) composite by batch technique. TUF was synthesized by methylation and condensation then alginate was immobilized to forms sol gel alginate beads, modifications of thiourea-formaldehyde sorption properties by incorporation of sorptive materials such as alginate to improve sorption performance of alginate through amine and thio groups of thiourea. The adsorbent was characterized by FTIR spectroscopy, X-ray diffraction, Scanning electron microscopy and energy dispersive spectroscopy (EDX). The influence of experimental parameters such as pH, initial dye concentration, contact time, temperature adsorbent dosage and ionic strength was investigated. Moreover, the adsorption isotherm, kinetic and thermodynamic of dye adsorption was studied. Further, the recovery of the dye from the adsorbent was also attempted.

2. Experimental setup

2.1. Chemicals and reagents

All chemicals which used were of analytical grade and demineralized water was used for the preparation of all aqueous solutions. Sodium alginate was purchased as alginic acid sodium salt (Fluka Co, Romania), acid dye Congo red was obtained from (Cromatos SRL, Italy), Basic dye crystal violet Sigma Aldrich (Switzerland), hydrochloric acid (HCl 35%), sodium hydroxide (NaOH 99.9%) and CaCl_2 were supplied by Merck Company (Germany). A stock solution whose concentration was $1 \times 10^{-3} \text{ M}$ was used and could be diluted to the required concentration with demineralized water in the experiment. Stock solution was prepared in distilled water and all the test solutions were prepared by diluting the stock with distilled water [9]. All chemical reagents are analytical grade and were used as received.

2.2. Physical measurements

In order to confirm the functionalization of the sorbent (TUFA) composite spectroscopic data of the investigated dye were obtained using the following instruments: Fourier transform infrared (FTIR) spectrophotometer spectra (KBr discs, $4,000\text{--}400 \text{ cm}^{-1}$) by Jasco-4100 spectrophotometer. The SEM results of the MSAB sample before and after the adsorption processes were obtained using (JEOL-JSM-6510 LV) scanning microscope to observe surface modification. The structure of the synthesized adsorbents was examined by X-ray diffraction measurement (XRD) is recorded on X-ray diffract meter in the range of diffraction angle $2\theta = 5^\circ\text{--}80^\circ$. The elemental distribution of TUFA was analyzed using the energy-dispersive X-ray spectroscopy (EDX) and taken on a Leo1430VP microscope with operating voltage 5 kV. The Brunauer-Emmett-Teller (BET) surface area and Barrett-Joyner-Halenda (BJH) pore volume which form N_2 adsorption/desorption isotherms on MSAB at 77 K measured on Quanta chrome Nova Instruments version 10 were calculated. UV-visible spectrophotometer (Perkin-Elmer AA800 Model AAS) was employed for absorbance measurements of samples. HANNA Instruments pH meter (model 211) used for pH adjustment and Maxturdy 30 (Wisd) for shaking.

2.3. Preparation of thiourea-formaldehyde encapsulated alginate

The producer of thiourea-formaldehyde with calcium alginate beads encapsulated resin (Fig. 1).

2.4. Adsorption experiments

Sorption experiments were performed in batch systems using polyethylene flasks and the temperature was set to $25^\circ\text{C} \pm 1^\circ\text{C}$. For the study of pH effect 25 mL of 100 mg.L^{-1} each dye solutions at different pH values in the range (1–12) were mixed with 0.05 mg for (CR) and 0.02 mg for (CV) solution of a concentration ($1 \times 10^{-4} \text{ M}$) of the TUFA sorbent (dried mass) for 90 s, the pH of the dyes solutions had been adjusted to values ranging from 1.0 to 10.0 for CR and 3.0 to 12.0 for CV by adding a few drops of aqueous HCl and NaOH solutions (0.01–0.1 M) to contact with the adsorbent. The pH of each suspension was measured using a pH meter. The Erlenmeyer flasks were transferred to a shaker water bath (Maxturdy 30 (Wisd)) at 25°C and mechanically stirred at 200 rpm until equilibrium. After shaking, the solid and liquid phases were separated by Filtration (Whatman filter paper $0.45 \text{ }\mu\text{m}$) and the concentration of dyes in the supernatant phase was analyzed for residual dye concentration and the sorption capacity (q_{eq} , mg.g^{-1}) was determined by the mass balance equation:

$$q_{\text{eq}} = (C_i - C_e) \times \frac{v}{m} \quad (1)$$

where C_i and C_e are the initial and equilibrium concentration of dye in solution (mmol.L^{-1}), respectively. V is the volume of solution (L) and m the mass of sorbent (g).

The main factors that play the key role for the dye–adsorbent interactions are charge and structure of dye, adsorbent surface properties, hydrophobic and

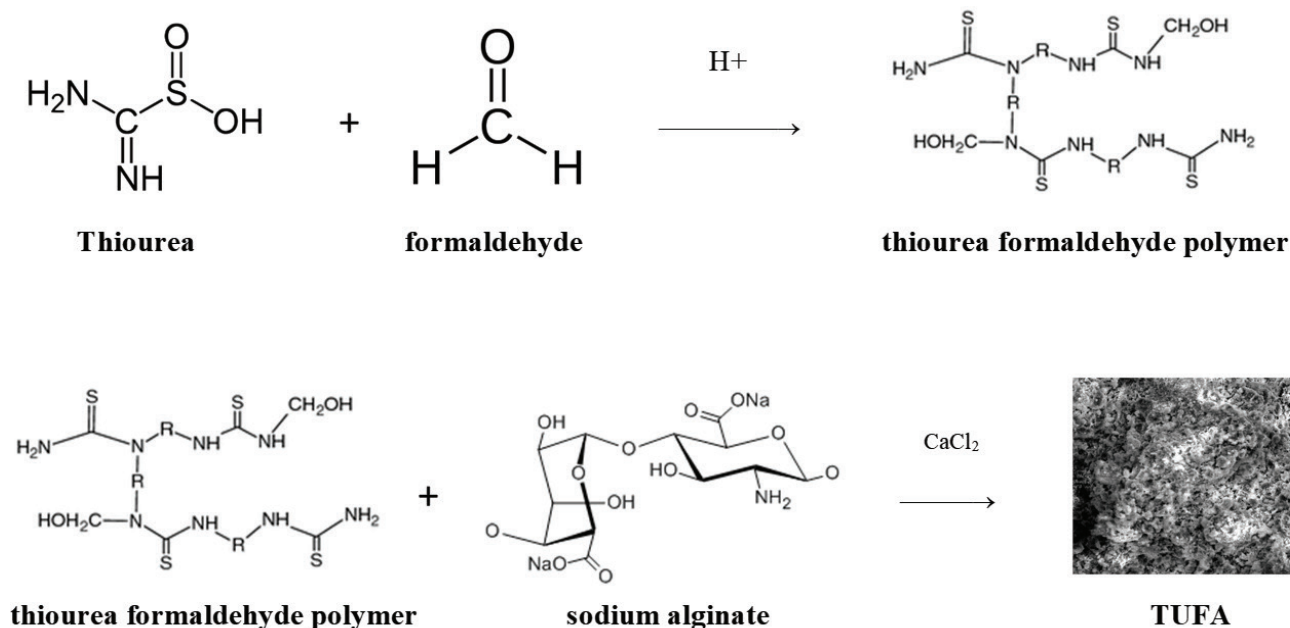


Fig. 1. Synthesis methods of the (TUFA) and mechanism of dye adsorption.

hydrophilic nature, hydrogen bonding, electrostatic interaction, steric effect and Vander Waals forces [10]. Equilibrium studies that give the capacity of the adsorbent and adsorbate are described by adsorption isotherms, which are usually the ratio between the quantity adsorbed and that remained in solution at equilibrium at fixed temperature [11]. The equilibrium relationships between adsorbent TUFA and adsorbate CR and CV are best explained by sorption isotherms. The present investigation deals with the applicability of Langmuir, Freundlich, Dubinin–Radushkevich (D–R), and Temkin adsorption isothermal models to the experimental data. For sorption isotherms 0.05 mg of sorbent (m) with (CR) and 0.02 mg of sorbent with (CV) were mixed with 25 mL (V) of each dye solution at different initial concentrations (C_i , ranging between 0.0001 and 0.005 M) for 90 s. The pH of the solutions was set at 5 and 9 for CR and CV, respectively. After solid/liquid adsorption, all samples were filtered through (Whatman) filter papers 0.45 nm to analysis. The residual concentration was determined in aqueous phase was analyzed using a double beam UV-visible spectrophotometer (Perkin-Elmer AA800 Model AAS) at 497 nm for CR and 590 nm for CV. Each experiment was carried out under identical conditions and value of the concentration of dyes in the supernatant phase was determined (C_e , mmol.L^{-1}) and the sorption capacity (q_{eq} , mg.g^{-1}) was determined by the mass balance Eq. (1). For uptake kinetics 0.3 g of sorbent were mixed with 150 mL of CR ($C_i = 2 \times 10^{-3}$ mmol.L^{-1}) at pH 5 and 0.12 g of sorbent were mixed with 150 mL of CV dye solutions ($C_i = 5 \times 10^{-4}$ mmol.L^{-1}) at pH 9. Samples (5 mL) were collected at fixed times and the residual concentrations were determined. The shaking speed was set at 200 rpm while the temperature was maintained at $25^\circ\text{C} \pm 1^\circ\text{C}$. Standard aqueous solutions of dye at each pH studied were prepared to build a calibration curve from which the

concentration of dyes was calculated. The amount of dye adsorbed onto the TUFA at each pH studied was calculated. In any adsorption process, both energy and entropy considerations must be taken into account in order to determine what process will occur spontaneously. Values of thermodynamic parameters are the actual indicators for practical application of a process. The chemical (chemisorption) or physical (Physisorption) adsorption mechanism is often an important indicator to describe the type of interactions between CR, CV and TUFA composite. The magnitude of activation energy gives an idea about the type of adsorption which is mainly physical or chemical. Low activation energies ($0\text{--}40$ kJ.mol^{-1}) are characteristics for Physisorption, while higher activation energies ($40\text{--}800$ kJ.Mol^{-1}) suggests chemisorption [12].

2.5. Desorption experiments

The regeneration of adsorbent is important and the adsorbents having regeneration ability are considered cost effective. Regeneration experiments were done by performing three consecutive cycles of adsorption/desorption using 25 ml of 0.1 M NaOH with 0.5 g of the loaded composite (TUFA-acidic dye) and 0.1 M HCl with 0.5 g of the loaded composite (TUFA-basic dye) for 30 s then the regeneration efficiency was estimated. After regeneration the regenerated sorbent was decanted and washed carefully by distilled water for reuse in the subsequent run. The efficiency of regeneration was calculated according to the following equation:

$$\text{Regeneration efficiency}(\%) = \frac{\text{Adsorption capacity in the second run}}{\text{Adsorption capacity in the first run}} \times 100 \quad (2)$$

3. Results and discussion

3.1. Characterization of adsorbents

The various constituents of TUFA per chemical and analytical techniques are applied and characterized with further analysis as: IR spectroscopy (FTIR). Scanning electron microscopic photographs revealed the absorptive nature of adsorbent. The presence of TUFA was examined by X-ray diffraction measurement (XRD) is recorded on X-ray diffractometer. The elemental distribution of TUFA was analyzed using the energy-dispersive X-ray spectroscopy (EDX).

3.1.1. Infra-red spectrometry

The FT-IR spectra of TUFA particles wave number range 4,000–400 cm^{-1} (Fig. 2) showed that the broad bands appearing in the range of 3,500–3,200 cm^{-1} can be attributed to the hydroxyl group (O–H stretching vibrations) of calcium alginate. The symmetric and asymmetric aliphatic C–H stretching bands were observed at 3,046.98 and 2,958.27 cm^{-1} , respectively. The bands at 1,608.34 and 1,546.63 cm^{-1} were attributed to the asymmetric and symmetric stretching vibrations of carboxylate group of alginates, respectively. The bands at 1,434.78 and 1,280.5 cm^{-1} were attributed to the C–O stretching vibration of pyranosyl ring and the C–O stretching with contributions from C–C–H and C–O–H deformations [13]. The peak at 1,145.51 cm^{-1} for C–O–C stretching was also seen with TUF resin. The bands at 960.37 cm^{-1} for thiourea functional group N–C–S stretching and at 744.38 cm^{-1} for C–S stretching. [14]. Thus, we inferred that thiourea-formaldehyde capsulated with alginate resin. The spectra of dye loaded TUFA sorbent has very similar FT-IR profiles the same bands are appearing on all spectra, the only small differences are observed, a small shift in some of these bands.

3.1.2. Scanning electron microscope (SEM)

Scanning electron microscopy has been a primary tool for characterizing the surface morphology and fundamental physical properties of the adsorbent surface. It is useful for determining the particle shape, porosity and appropriate size distribution of the adsorbent [15]. Scanning electron micrographs of raw TUFA are shown in Fig. 3. A granular material coating on TUFA has considerable numbers of pores where, there is a good possibility for dyes to be trapped and adsorbed into these pores.

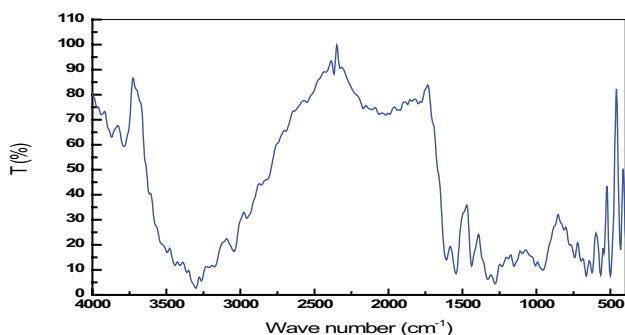


Fig. 2. FT-IR spectrum of the (TUFA) adsorbent.

3.1.3. X-ray diffraction (XRD) analysis

XRD analysis (Fig. 4) was used for characterizing the crystalline structure of the material, which is induced by the magnetite core. The XRD pattern shows a limited number of peaks characteristics of iron oxides may be identified. The large fraction of polymer may contribute to explain the poor resolution of the XRD pattern. The peaks characteristics of TUFA [16] are usually identified at indices: 16.8 (98), 21.94 (158), 43.96 (70), 64.3 (54) and 77.42 (70).

3.2. Batch adsorption analysis

The amount of dye that can be removed from solution by sorbent (q_e) was depend on process variables used in batch system such as pH values, initial dye (CR, CV) concentrations, contact time, solution temperatures, adsorbent dose and ionic strength. Dye–dye interactions also play an important role between dye and aqueous solution, Congo red, is an anionic azo dye having IUPAC name as 1-naphthalene sulfonic acid, 3,3-(4,4-biphenylenebis(azo)) bis (4-amino disodium) salt. The maximum wavelength (λ_{max}) in the absorption spectrum is 497 nm [17]. Crystal violet (CV) is a cationic dyes also known as basic violet and methyl violet. Its IUPAC name is 4-[Bis[4-(dimethyl amino)phenyl]methylene] -N,N-dimethyl-2,5-cyclohexadien-1-iminium chloride}. The maximum wavelength (λ_{max}) in the absorption spectrum is 590 nm. Chemical properties of both dyes including its molecular formula, molecular weight, molecular structure and maximum wavelength (λ_{max}) are reported in Tables 1 and 2.

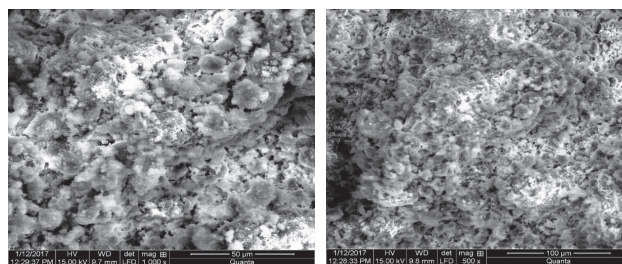


Fig. 3. Scanning electron micrographs of unloaded (TUFA).

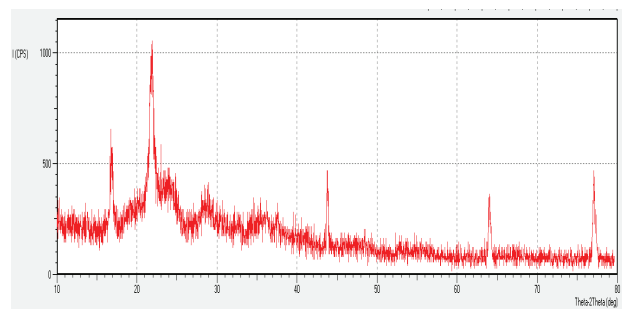


Fig. 4. Powder X-ray diffraction (XRD) pattern of (TUFA) particles.

Table 1
Properties of the adsorbate (CR) anionic dye

Parameter	Characteristic
Name	Congo red
Symbol	CR
Type color	Anionic
Chemical formula	$C_{32}H_{22}N_6Na_2O_6S_2$
Molecular weight (g/mol)	696.66
Wavelength of maximum absorption (nm)	497
Molar extinction coefficient, ϵ_{497} ($M^{-1} cm^{-1}$)	$6.26 \times 10^4 M^{-1} cm^{-1}$
Chemical structure of color	

Table 2
Properties of the adsorbate (CV) cationic dye

Parameter	Characteristic
Name	Crystal violet
Symbol	CV
Type color	Cationic
Chemical formula	$C_{25}H_{30}N_3Cl$
Molecular weight (g/mol)	407.98
Wavelength of maximum absorption (nm)	590
Molar extinction coefficient, ϵ_{590} ($M^{-1} cm^{-1}$)	$8.7 \times 10^4 M^{-1} cm^{-1}$
Chemical structure of color	

3.2.1. Effect of pH

pH is an important parameter controlling the solid–liquid adsorption that can affect the surface charge of the adsorbent functional groups and the ionization degree of the adsorbate. Maximum adsorption was observed at pH 5.0 for CR and pH 9.0 for CV. Though, the pH value of the dye solution will affect the overall adsorption behavior and mechanism. At pH_{pzc} the adsorbent has zero potential charge on its surface, the pH_{pzc} of TUFA is about 7. Theoretically at pH higher than pH_{pzc} adsorbent surface get negative charge and at lower pH get positive charge, based on electrostatic interaction between dye and adsorbent (Fig. 5). The view in the adsorption of CR by TUFA was investigated at initial pH value show no presumed change was observed for CR adsorption onto TUFA in this pH range. The final pH_{sat} adsorption equilibrium,

were found to reach constant value of 5.0. This indicates that TUFA has a strong buffering ability [18]. In this pH increases gradually the concentration of H^+ ions in the system lead to increase amount of CR exist in water as anions (CR^-) and the surface of TUFA still positively charged ($pH < pH_{pzc}$), this behavior can be explained by the electrostatic interactions between protonated adsorption sites of the adsorbent and negatively charge dye ions in addition to hydrogen bonding interaction at $pH < pH_{pzc}$ [19], while In case of CV adsorption, at $pH > pH_{pzc}$ the surface is negatively charged the higher percentage removal at higher pH may be due to chemical reaction between the sorbent and dye, the electrostatic attraction between the positively charged dye molecules and the negatively charged adsorption sites of the adsorbent to evaluate the effect of pH on the surface characteristics of the adsorbent and its adsorption behavior, As the pH of the

system increases, the number of negatively charged sites on the adsorbent surface increases and the number of positively charged sites decreased. A negatively charged surface site on the adsorbent does not favor the adsorption of dye anions due to the electrostatic repulsion [20]. Also, lower adsorption of CR at alkaline pH is due to the presence of excess OH⁻ ions competing with the dye anions for the adsorption sites. Conversely trend was observed for CV adsorption.

3.2.2. Adsorption isotherms

The adsorption isotherm indicates the adsorbing molecules distribute between liquid phase and solid phase. The adsorption experimental data obtained in this study were analyzed by the commonly used Langmuir, Freundlich, Dubinin–Radushkevich (D–R) and Temkin isotherm models. A correct fit for Langmuir model is observed in Fig. 6. Fig. S1 (see supplementary material) shows the results of the adsorption equilibrium experiments of both dyes and data fitted to the linear Langmuir equation at different temperature.

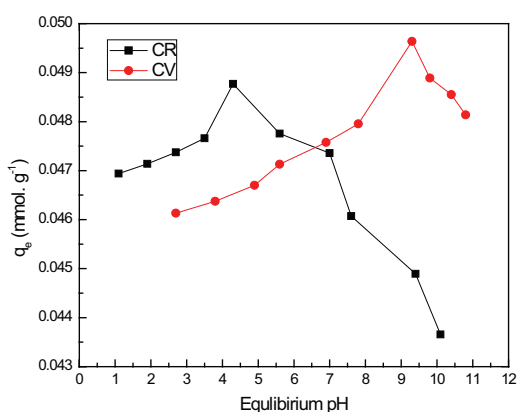


Fig. 5. Effect of pH solution for removal of CR and CV on (0.05 and 0.02 g) of (TUFA) respectively at 25°C ± 1°C.

The calculated parameters of Langmuir, Freundlich, Dubinin–Radushkevich (D–R) and Temkin are reported in Table 3. According to the values of R_2 listed in Table 3, Langmuir model is best to fit the adsorption equilibrium data while Freundlich model is not suitable to fit process.

3.2.2.1. Langmuir isotherm The Langmuir adsorption, which is the monolayer adsorption, depends on the assumption that the intermolecular forces decrease rapidly with distance and consequently predicts the existence of monolayer coverage of the adsorbate at the outer surface of the adsorbent. The saturated or monolayer capacity can be represented as the known linear form of Langmuir equation that described by the following equation [21]:

$$\frac{C_e}{q_e} = \frac{1}{q_{\max}K_L} + \frac{C_e}{q_{\max}} \quad (3)$$

where C_e is the equilibrium dye concentration in solution (mg.L⁻¹), q_e is the equilibrium dye concentration in the adsorbent (mg.g⁻¹), q_{\max} is the monolayer capacity of the adsorbent (mg.g⁻¹) and K_L is the Langmuir adsorption constant (L.mg⁻¹). Therefore, a plot of C_e/q_e vs. C_e (Fig. 6(a)) gives a straight line of slope $1/q_{\max}$ and the intercept $1/(q_{\max}K_L)$. The maximum monolayer adsorption capacity and the Langmuir constant were found to be 559.55 mg.g⁻¹ and 18.86 L.mg⁻¹ for CR and 237.77 mg.g⁻¹ and 165.91 L.mg⁻¹ for CV. High R^2 values (0.9968 for CR and 0.9995 for CV) of the straight lines obtained confirm the validity of Langmuir adsorption isotherm for adsorbent.

The dimensionless parameter of equilibrium, separation factor 'r' suggested by Adam and Chua, Weber and Chakrabarti [22] can be calculated as:

$$r_L = \frac{1}{1 + K_L C_0} \quad (4)$$

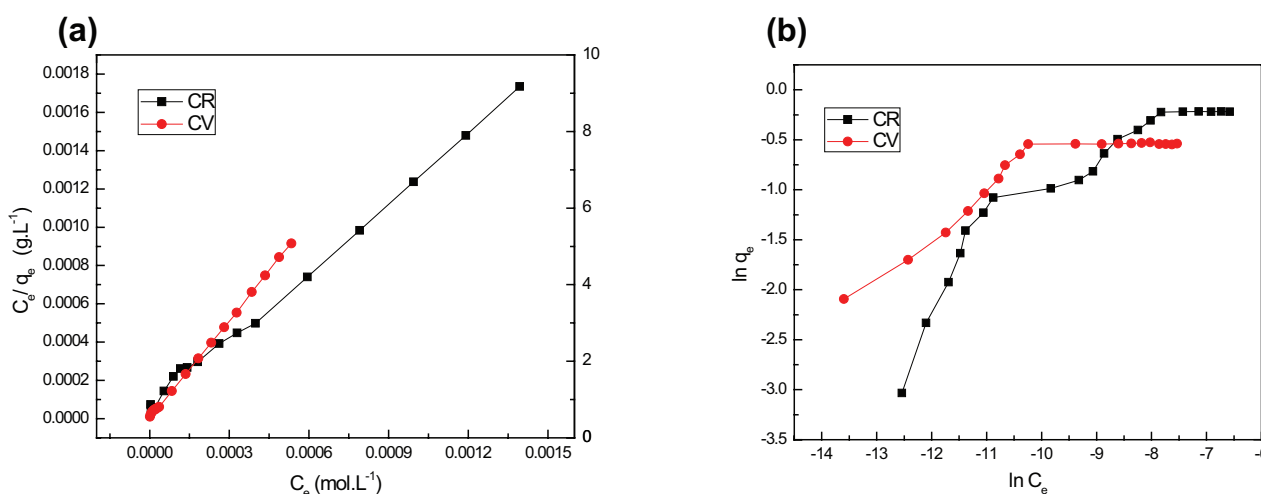


Fig. 6. Adsorption isotherm for removal of CR and CV on (0.05 and 0.02 g) of (TUFA) respectively at 25°C ± 1°C.

Table 3
Isotherm model parameters for the adsorption of CR and CV onto TUFA

Isotherm	Equation		Value of parameters		
			Parameter	CR	CV
Langmuir	$\frac{C_e}{q_e} = \frac{1}{q_m K_L} + \frac{C_e}{q_m}$	The constants q_m and K_L are calculated by the plot of C_e/q_e vs. C_e with slope $1/q_m$ and intercept $1/(q_m K_L)$	$q_{e \text{ exp}} (\text{mg}\cdot\text{g}^{-1})$	559.55	237.77
			$q_e (\text{mg}\cdot\text{g}^{-1})$	586.93	241.44
			$K_L (\text{L}\cdot\text{mg}^{-1})$	18.87	165.91
			R^2	0.9968	0.9995
Freundlich	$\ln q_e = \ln K_F + \frac{1}{n} \ln C_e$	K_F and n can be calculated from a linear plot of $\ln q_e$ against $\ln C_e$	n	2.62	4.41
			$K_F (\text{L}\cdot\text{mg}^{-1})$	13.62	3.95
			R^2	0.8544	0.7737
Dubinin–Radushkevich	$\ln q_e = \ln Q_{\text{DR}} - K_{\text{DR}} \varepsilon^2$	The slope of the plot of $\ln q_e$ vs. ε^2 gives $K_{\text{DR}} (\text{mol}^2 (\text{kJ}^2)^{-1})$ and the intercept yields the adsorption capacity, $Q_{\text{DR}} (\text{mg}\cdot\text{g}^{-1})$	$Q_{\text{DR}} (\text{mg}\cdot\text{g}^{-1})$	636.81	121.25
			$K_{\text{DR}} (\text{mol}^2 (\text{kJ}^2)^{-1})$	-3.335E-09	-1.879E-09
			R^2	0.8940	0.8337
			$E (\text{kJ}\cdot\text{mol}^{-1})$	1.22	1.63
Temkin	$q_e = \beta_T \ln K_T + \beta_T \ln C_e$	The parameters B_T and K_T are the Temkin constants that can be determined by the plot of q_e vs. $\ln C_e$	β_T	182	3.13
			$K_T (\text{L}\cdot\text{mg}^{-1})$	12.93	15.71
			R^2	0.9617	0.8208
			$b (\text{kJ}\cdot\text{mol}^{-1})$	0.1362	0.079

where C_0 is the initial concentration and K_L signifies the Langmuir constant. There are four probabilities for the value of r : (i) for favorable adsorption, $0 < r < 1$, (ii) for unfavorable adsorption, $r > 1$, (iii) for linear adsorption, $r = 1$, and (iv) for irreversible adsorption, $r = 0$. The obtained values of separation factor are 0.042, 0.036, 0.032 and 0.28 for TUFA with CR and 0.0099, 0.0091, 0.0085 and 0.0179 for TUFA with CV at 25°C, clearly indicating the favorability of the adsorption process.

3.2.2.2. Freundlich isotherm The Freundlich isotherm is a result of the assumption that the adsorption occurs on a heterogeneous surface and non-uniform distribution of the heat of adsorption over the adsorbent surface takes place, characterized by the heterogeneity factor $1/n$, describes reversible adsorption and is not restricted to the formation of the monolayer. The empirical Freundlich model which is known to be satisfactory for low concentrations is expressed by the equation:

$$q_e = K_F C_e^{1/n} \quad (5)$$

where q_e is the equilibrium dye concentration on adsorbent ($\text{mg}\cdot\text{g}^{-1}$), C_e is the equilibrium dye concentration in solution ($\text{mmol}\cdot\text{L}^{-1}$), K_F is Freundlich constant ($\text{mg}\cdot\text{g}^{-1}$) and $1/n$ is the heterogeneity factor. A linear form of the Freundlich expression can be obtained by taking Anti logarithms of the equation:

$$\ln q_e = \ln K_F + \frac{1}{n} \ln C_e \quad (6)$$

The plot of $\log q_e$ vs. $\log C_e$ (Fig. 6(b)) for the adsorption of CR and CV onto TUFA composite was employed to generate the intercept value of K_F and the slope of $1/n$.

One of the Freundlich constants K_F indicates the adsorption capacity of the adsorbent, the other Freundlich constant n is a measure of the deviation from linearity of the adsorption. The value of n is an indication of the favorability of adsorption. If a value for n is equal to unity the adsorption is linear. If a value for n is below unity, this implies that adsorption process is chemical, but a value for n is above unity, represent favorable nature of adsorption [23].

The highest value of n at equilibrium is 2.62 for CR and 4.41 for CV (Table 3), represents favorable adsorption and therefore this would seem to suggest that the adsorption is physical, which is referred the adsorption bond becomes weak and conducted with Vander Waals forces rather than chemical adsorption.

3.2.2.3. Dubinin–Radushkevich isotherm The linear form of the Dubinin–Radushkevich isotherm [24] is expressed as:

$$\ln q_e = \ln Q_{DR} - K_{DR} \varepsilon^2 \quad (7)$$

where q_e is the amount of the dye adsorbed per unit weight of the adsorbent (mg.g^{-1}), Q_{DR} is the maximum sorption capacity provided by the intercept in (mol.G^{-1}), K_{DR} ($\text{mol}^2.\text{J}^{-2}$) is obtained from the slope of the straight-line plot of $\ln q_e$ vs. ε^2 . Fig. S2(a) (see supplementary material) presents a straight line with regression coefficients almost unity is obtained and ε , can be calculated as:

$$\varepsilon = RT \ln \left(1 + \frac{1}{C_e} \right) \quad (8)$$

where ε is the Polanyi potential, R is the gas constant 8.314 kJ/mol K , T is the temperature (K) and C_e is the dye equilibrium concentration. The mean free energy of sorption E (kJ/mol) required to transfer one mole of dye from the infinity in the solution to the surface of TUFA can be determined by the following equation:

$$E = \frac{1}{\sqrt{-2K_{DR}}} \quad (9)$$

The value of E is very useful in predicting the type of adsorption and if the value is less than 8 kJ.mol^{-1} , the adsorption is physical in nature and if it is in between $8\text{--}16 \text{ kJ.mol}^{-1}$, the adsorption is related to ions exchange. The values of E for (dye–TUFA) was found 1.22 kJ.mol^{-1} for CR and 1.63 kJ.mol^{-1} for CV, suggesting that Physisorption is responsible for the adsorption process for both systems (Table 3).

3.2.2.4. Temkin isotherm The Temkin isotherm assumes that the heat of adsorption of all the molecules increases linearly with coverage [25] Plots between $\ln C_e$ vs. q_e for TUFA gave straight lines at 25°C (Fig. S2(b)), supplementary material), there verifying the Temkin isotherm in the adsorption of dye ion over adsorbent. Slopes and intercepts of these straight lines help to determining the values of Temkin constants values (Table 3). The linear form of this isotherm can be given as:

$$q_e = \beta_T \ln K_T + \beta_T \ln C_e \quad (10)$$

where q_e is the amount adsorbed at equilibrium in (mmol. G^{-1}), k_T is the Temkin isotherm bonding energy

constant in (L.mmol^{-1}) and β_T is the constant related to the heat of adsorption and it is defined by the expression:

$$\beta = \frac{RT}{b} \quad (11)$$

where b is the variation of the adsorption energy, R is the universal gas constant (8.314 kJ/mol K), T is the temperature (K) and K_T is the equilibrium binding constant corresponding to the maximum binding energy. Typical bonding energy range for ion exchange mechanism is reported to be in the range of $8\text{--}16 \text{ kJ/mol}$ while physisorption processes are reported to have adsorption energies less than 40 kJ/mol . Very low values of b ($0.1362 \text{ kJ.mol}^{-1}$ for CR and $0.079 \text{ kJ.mol}^{-1}$ for CV) obtained in the present study indicates rather weak ionic interaction between the sorbate and the present sorbent and the dye removal seems to involve physisorption.

3.2.3. Adsorption kinetic studies

The study of adsorption kinetics describes the solute uptake rate and evidently this rate controls the residence time of adsorbate uptake at the solid–solution interface. The uptake of CR and CV increased with contact time (Fig. 7). The rate of removal of CR and CV by adsorption was rapid initially and then slowed gradually until it attained an equilibrium beyond which there was significant increase in the rate of removal irrespective of their initial dyes concentrations (Figs. S3 and S4). The maximum adsorption onto TUFA composite was observed at 60 min for CR and 30 min for CV and it is mean as the equilibrium time. Over evaluating the adsorption kinetics of CR and CV onto TUFA composite, the pseudo-first-order and pseudo-second-order kinetic models were used to fit the experimental data, according to the below kinetic model equations. The pseudo-first-order rate expression of Lagergren equation [26] is given as:

$$\log(q_e - q_t) = \log q_e - \left(\frac{K_1}{2.303} \right) t \quad (12)$$

The pseudo-second-order kinetic model is expressed as:

$$\frac{t}{q_t} = \frac{1}{K_2 q_e^2} + \left(\frac{1}{q_e} \right) t \quad (13)$$

where q_t is the amount of dye adsorbed (mmol.g^{-1}) at various times t , q_e is the maximum adsorption capacity (mmol.g^{-1}) for pseudo-first-order adsorption, k_1 is the pseudo-first-order rate constant for the adsorption process (min^{-1}), q_e is the maximum adsorption capacity (mmol.g^{-1}) for the pseudo-second-order adsorption, k_2 is the rate constant of pseudo second-order adsorption ($\text{g.mol}^{-1}.\text{min}^{-1}$). The straight-line plots of $\log(q_e - q_t)$ vs. t for the pseudo-first-order reaction and t/q_t vs. t for the pseudo-second-order reaction (Figs. 7(a) and (b)) for adsorption of CR and CV onto TUFA composite have also been tested to obtain the rate parameters. The k_1 , k_2 , q_e , q_t , and correlation coefficients and R^2 for both CR and CV under different temperatures were

calculated from these plots and are given in Table 4. The correlation coefficients (R^2) for the pseudo-first-order kinetic model are less than the value of correlation coefficient (R^2) for the pseudo-second-order kinetic model for both dyes. It is probable, therefore, that this adsorption system is not a pseudo-first-order reaction; it fits the pseudo-second-order kinetic model.

3.2.4. Thermodynamic parameters

The effect of temperature on the sorption of CR and CV onto TUFA was studied by performing the adsorption experiments at different temperature (293–318 K). The positive value of ΔH° is suggestive of an endothermic nature which favors the adsorption of two dyes at higher temperature.

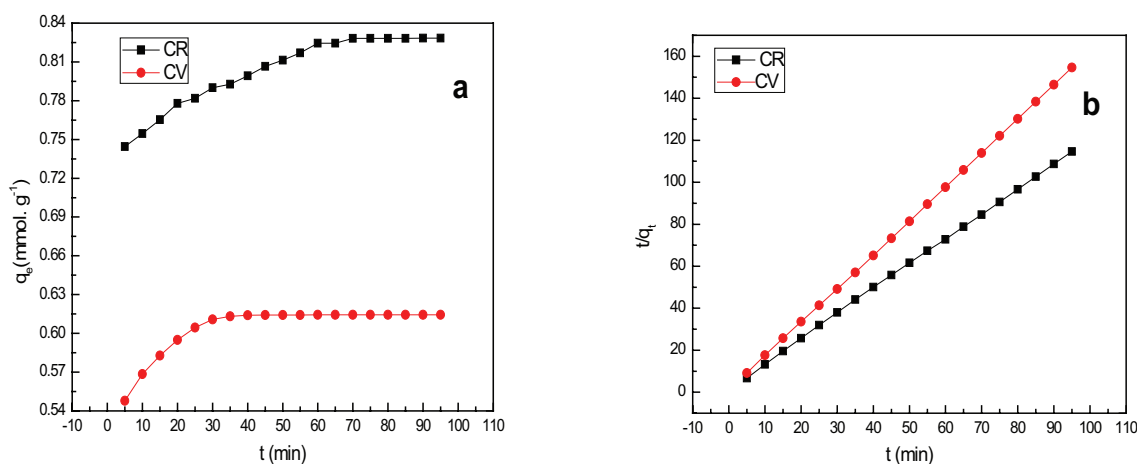


Fig. 7. Adsorption kinetics (a) PFORE, (b) PSORE for removal of CR and CV on (0.05 and 0.02 g) of (TUFA) respectively at $25^\circ\text{C} \pm 1^\circ\text{C}$.

Table 4
Kinetics parameters for the adsorption of CR and CV onto TUFA

Model	Equation		Value of parameters		
			Parameter	CR	CV
Pseudo-First-order kinetic	$\log(q_e - q_t) = \log q_e - \left(\frac{K_1}{2.303}\right)t$	The plot of $\ln(q_e - q_t)$ against t gives a straight line with the slope $-k_1$ and intercept $\ln q_e$	k_1 (min^{-1})	-0.0407	-0.0442
			q_e ($\text{mg}\cdot\text{g}^{-1}$)	347.14	18.08
			R^2	0.8739	0.9564
Pseudo-second-order kinetic	$\frac{t}{q_t} = \frac{1}{K_2 q_e^2} + \frac{t}{q_e}$	Values of k_2 and q_e for different initial concentrations of dye were calculated from the slope and intercept of the linear plot of t/q_t vs. t	k_2 (min^{-1})	0.7374	2.5793
			q_e ($\text{mg}\cdot\text{g}^{-1}$)	587.14	252.82
			R^2	0.9998	0.9999
Intraparticle diffusion	$q_t = K_i t^{1/2} + X$	The parameters K_i and X were determined from the linear plot of q_t vs. $t^{1/2}$	K_i ($\text{mg}\cdot\text{g}^{-1}\cdot\text{min}^{-1/2}$)	8.42	2.83
			X ($\text{mg}\cdot\text{g}^{-1}$)	502.64	227.74
			R^2	0.9616	0.6607
Elovich	$q_t = \frac{1}{\beta} \ln(\alpha\beta) + \frac{1}{\beta} \ln t$	The constants α and β were obtained from the slope and intercept of a line plot of q_t vs. $\ln t$	B ($\text{g}\cdot\text{mg}^{-1}$)	20783	19127
			A ($\text{mg}\cdot\text{g}^{-1}\cdot\text{min}^{-1}$)	1374	690.6
			R^2	0.9670	0.8351

Adsorption process is generally considered as physical if $\Delta H^\circ < 25 \text{ kJ.Mol}^{-1}$ and as chemical when $\Delta H^\circ > 40 \text{ kJ.Mol}^{-1}$. The positive value of entropy (ΔS°) is suggestive of higher randomness of adsorption in the system and favors the stability of the adsorption. The negative values of (ΔG°) for these processes confirm the feasibility and spontaneous nature of adsorption process. As shown in Table 5, with increasing temperature, there are more adsorption efficient of CR and CV. The amount of CR and CV adsorbed onto TUFA composite at equilibrium and at different temperatures (20°C, 25°C, 30°C, 35°C, 40°C and 45°C) has been examined to obtain thermodynamic parameters for the adsorption system. The determination of thermodynamic parameters, Gibb's free energy (ΔG°), change in entropy (ΔS°) and change in enthalpy (ΔH°) were calculated using the following relations:

$$K_c = \frac{C_e}{C_s} \tag{14}$$

$$\Delta G^\circ = -RT \ln K_c \tag{15}$$

$$\Delta G^\circ = \Delta H^\circ - T \Delta S^\circ \tag{16}$$

$$\ln K_c = \frac{\Delta S^\circ}{R} - \frac{\Delta H^\circ}{RT} \tag{17}$$

where K_c is the equilibrium constant, C_e is the amount of CR and CV adsorbed on the TUFA composite of the

solution at equilibrium (mol.L^{-1}), C_s is the equilibrium concentration of the dyes in the solution (mol.L^{-1}). The K_2 of the pseudo-second-order model in Table 4 was used to obtain C_e and C_s . T is the solution temperature (K) and R is the gas constant, ΔH° and ΔS° were calculated from the slope and the intercept of Van't Hoff plots of $\ln K_c$ vs $1/T$ (Fig. 8(b)). The positive values of both entropy and enthalpy show the increased randomness and endothermic nature of the process, respectively, whereas the negative values of free energy suggest the feasibility of the process, thereby demonstrating that the process is stable energetically [27].

The pseudo-second order rate constant of CR and CV adsorption is expressed as a function of temperature by the following Arrhenius type relationship [28]:

$$\ln K_2 = \ln A - \frac{E_a}{RT} \tag{18}$$

where E_a is the Arrhenius activation energy of adsorption, A is the Arrhenius factor, R is the gas constant and is equal to $8.314 \text{ J.mol}^{-1} \text{ K}^{-1}$ and T is the operating temperature in Kelvin. A linear plot of $\ln K_2$ vs. $1/T$ for the adsorption of CR and CV onto TUFA composite (Fig. 8(a)) was constructed to generate the activation energy from the slope ($-E_a/R$). The result of activation energy obtained is 1.13 kJ.mol^{-1} for CR and 3.51 kJ.mol^{-1} for CV (Table 5) for the adsorption onto TUFA composite. The value of activation energy (E_a) for adsorption of both dyes by TUFA has a low potential and corresponds to a physisorption and is much temperature sensitive.

Table 5
Standard enthalpy, entropy and free energy changes for adsorption

Dyes	ΔH° (kJ.mol ⁻¹)	ΔS° (J.mol ⁻¹ K ⁻¹)	E_a (kJ.mol ⁻¹)	ΔG° (kJ.mol ⁻¹)					
				293 K	298 K	303 K	308 K	313 K	313 K
CR	1.58	0.0171	1.13	-6.6	-6.69	-6.78	-6.86	-6.95	-7.04
CV	20.04	0.1099	3.51	-52.25	-52.8	-53.3	-53.9	-54.45	-55.0

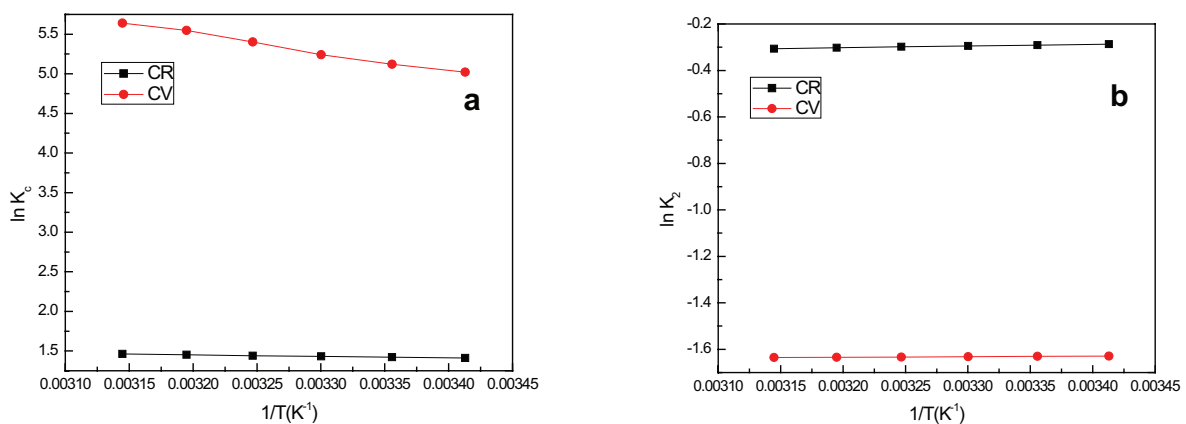


Fig. 8. Thermodynamic plots (a) Van't Hoff, (b) Arrhenius for removal of CR and CV on (0.05 and 0.02 g) of (TUFA) respectively.

3.2.5. Effect of adsorbent dose

The adsorption of CR and CV on the TUFA sorbent was studied by changing the quantity of adsorbent range of 0.01–0.1 g 25 mL⁻¹, with the dye concentration of 2×10^{-3} M and pH 5.0 for CR and 5×10^{-4} M pH 9.0 for CV at $25^\circ\text{C} \pm 1^\circ\text{C}$. The results in Figs. S5(a) and (c) (see supplementary material) show the CR adsorption capacity as a function of adsorbent amount. It has been found that the adsorption capacity decreases from 3.98 to 0.24 mmol.g⁻¹ for CR and from 1.13 to 0.12 mmol.g⁻¹ for CV when the dose of TUFA increases from 0.01 to 0.1 g 25 mL⁻¹. Figs. S5(b) and (d) (see supplementary material) shows the effect of dose on the equilibrium concentration (C/C_0) of dyes by the TUFA sorbent. As the dose increases, the equilibrium concentration of CR and CV is decreased, which is due to the increase in the adsorbent surface area of the adsorbent. The results shown indicate that the removal efficiency increases up to 99.1% ($C/C_0 = 0.156$) for CR and 97.3% ($C/C_0 = 0.024$) for CV at adsorbent dose of 0.1g 25 mL⁻¹. The surface of the adsorbent is composed of active sites with a spectrum of binding energies [29]. At the low dose of adsorbent, all of the sites are exposed entirely and the adsorption on the surface is saturated faster showing a higher adsorption capacity. An increase in the mass of adsorbent leads to a decrease in equilibrium adsorption capacity per unit weight of the adsorbent (q_e) because there is excess adsorbent for the limited amount of dye ions in the solution. According to the result, the dose of 0.01 g 25 mL⁻¹ will achieve the maximum loading capacity for the sorbent, and the dose of 0.1 g 25 mL⁻¹ will achieve the maximum removal efficiency. So, the determination of the optimum adsorbent dose depends on the design and purpose of treatment process. Thus, if the water quality standard set by who is the target, a larger amount of adsorbent is better (0.1 g 25 mL⁻¹), and if the maximum loading of the sorbent per unit mass is the target, the dose of 0.01 g 25 mL⁻¹ is more suitable (Fig. S5, supplementary material). A further increase in dosage yielded an almost constant percentage removal which may be attributed to the saturation of binding sites due to aggregation of adsorbed particles. According to these results, it is inferred that percentage removal of dye increases with sorbent concentration reaches a maximum and remains almost constant with further increase in dosage.

3.2.6. Effect of ionic strength

The effect of ionic strength (NaCl concentration) was investigated on the adsorption of CR⁻ and CV⁺ onto the composite. The observed adsorption capacities of the sorbent for two dyes were not largely affected with the increasing concentration of NaCl from 10–40 g.L⁻¹. This indicates that the adsorption of CR⁻ and CV⁺ onto the prepared composite was ionic strength-independent and similar results have been reported elsewhere [30]. This feature expands the potential application of TUFA as an effective adsorbent in dye containing waste with varying ionic strengths since there was no competition between the metal ions (Na⁺) and the functional groups of the CV⁺ molecules. The effect of ionic strength on adsorption of the two dyes onto the TUFA was investigated. CR and CV adsorption data under ionic strengths from

(10–40 g.L⁻¹ as NaCl) are shown in Fig. S6 (see supplementary material). In the entire experimental (pH 5.0 for CR and pH 9.0 CV), CR and CV adsorption data under different value of ionic strengths overlapped, indicating that ionic strength can hardly impact the adsorption of CR and CV onto TUFA. This also further confirmed that the surface electrostatic effect had no influence on the overall adsorption of both dye on TUFA.

3.3. Desorption studies

Desorption studies help to elucidate the mechanism and recovery of the adsorbate and adsorbent. TUFA composite was washed three times using 0.01 M NaOH solution at pH around 12 for CR and 0.01 M HCl at pH around 1, then filtered and left to be dried at 50°C in an oven overnight and stored on desiccator prior to reuse in the adsorption again. The removal of dye by adsorption on the adsorbent TUFA was compared before and after recovering process at the same conditions: (C_0 : 2×10^{-3} M; T : $25^\circ\text{C} \pm 1^\circ\text{C}$; pH 5) for CR and (C_0 : 5×10^{-4} M; T : $25^\circ\text{C} \pm 1^\circ\text{C}$; pH 9) for CV. First for CR as the pH of desorbing solution was increased, the percent of desorption increased, the number of negatively charged sites increased and negatively charged site on the adsorbent favors the desorption of dye anions due to the electrostatic repulsion. At pH 11, a significantly high electrostatic repulsion exists between the negatively charged surface of the adsorbent and anionic dye. Secondly for CV as the pH of desorbing solution was decreased, the percent of desorption increased, the number of positively charged sites increased. And positively charged site on the adsorbent favors the desorption of dye cations due to the electrostatic repulsion. The regeneration efficiency for each adsorption/desorption cycle was found to be 99.1%, 87.4%, 75.2% for CR and 97.3%, 84.8%, 76.7% for CV This indicates that composite has good performance for repeated use up to at least three times.

3.4. Comparison of adsorption of CR and CV dye with various sorbents

The result of experiments demonstrated using TUFA as adsorbent, is effective than other adsorbent for removal of CR and CV from aqueous solution. (Table 6) shows the comparison of maximum sorption capacities of the TUFA with a series of values found in the literature (together with the best operating conditions reported by respective authors). The TUFA adsorbent has a adsorption capacity of the same order of magnitude as other sorbents; although the bio glass nanospheres (BGN) [31], (CABI nano-goethite) [32], (Mg–Al–LDH) [33], PEI modified wheat straw (MWS) [34], CTAB modified wheat straw (MWS) [35], bentonite–alginate composite[36], poly(acrylamide-co-maleicacid)montmorillonite nanocomposites [37], and agricultural waste corncob [38] showed better adsorption capacity. It is noteworthy that the TUFA sorbent has an important advantage related to their fast kinetics. The high sorption capacity of the TUFA adsorbents toward CR and CV dye reveal that adsorbent could be promising for practical application in two dye removal from waste water.

Table 6
Comparison of sorption capacity for CR and CV dye with various adsorbents

Adsorbent material	Dye	Initial pH	Contact time (min)	Temperature (°C)	Sorption capacity (mg.g ⁻¹)	References
BGN	CR	7	80	50	54.3	[31]
CABI nano-goethite	CR	3	180	30	137.7	[32]
Mg–Al–LDH	CR	7.7	20	55	65	[33]
PEI modified wheat straw (MWS)	CR	5.0	300	40	104	[34]
CTAB modified wheat straw (MWS)	CR	5.0	300	35	665	[35]
Bentonite–Alginate Composite	CV	5.5	120	70	601.93	[36]
P(AAm-MA)/MMT nanocomposite	CV	7	180	20	20.48	[37]
Corncob	CV	7	240	26	2.49	[38]
TUFA	CR	5	60	25	559.5	[This work]
	CV	9	30	25	237.7	

4. Conclusion

TUFA prepared by condensation of thiourea with formaldehyde mixing with alginate in CaCl₂ solution through polymerization for the removal of both CR and CV dyes from aqueous solutions. TUFA was characterized by FTIR, SEM, XRD, EDX and BET (pore volume surface area) analysis. Experimental results showed that TUFA had a higher capacity to adsorb CR and CV. The results showed that the adsorption of the two dyes on the composite particles was affected by the initial pH value, the initial dye concentration, contact time and the temperature. Equilibrium experiments fitted well the Langmuir isotherm model and the maximum monolayer adsorption capacity for the CR dye was 559.55 and 237.77 mg.g⁻¹ for CV. Both kinetics and thermodynamic parameters of the adsorption process were estimated. These data indicated an endothermic spontaneous adsorption process that kinetically followed the pseudo-second-order adsorption process. The equilibrium data fitted well the Langmuir isotherm equation indicating the heterogeneity of the adsorbent surface. The Langmuir isotherm fit to the data specified the presence of two different natures of adsorption sites with different binding energies on the TUFA surface. Kinetic modelling showed that the adsorption behavior and mechanism of both dyes is believed to happen via surface adsorption till the surface functional active sites were entirely occupied subsequently, this behavior could be active for CR and CV due to the kinetic adsorption in the first few minutes was faster. It was found that the main adsorption mechanisms involved in the removal process are hydrogen bonding and electrostatic attraction. The results showed that TUFA could be promising adsorbent for two dyes removal because of their availability. In addition, the mean adsorption energy revealed that the adsorption process might be due to the dual nature of the process, physisorption and chemisorption, and was predominant on the chemisorption process. The templated composite particles could be regenerated through the desorption of the dye in pH 12.0 of NaOH for CR and pH 1.0 of HCl for CV solution and could be reused to adsorb the dye again. Adsorption capacity and the equilibrium time of the presented adsorbent were encouraging in comparison with many other reported adsorbents for the removal of both dyes.

References

- [1] Z. Jia, Z. Li, S. Li, Y. Li, R. Zhu, Adsorption performance and mechanism of methylene blue on chemically activated carbon spheres derived from hydrothermally prepared poly (vinyl alcohol) microspheres, *J. Mol. Liq.*, 220 (2016) 56–62.
- [2] C. Yang, L. Li, J. Shi, C. Long, A. Li, Advanced treatment of textile dyeing secondary effluent using magnetic anion exchange resin and its effect on organic fouling in subsequent RO membrane, *J. Hazard. Mater.*, 284 (2015) 50–57.
- [3] C. Zhou, Q. Wu, T. Lei, I.I. Negulescu, Adsorption kinetic and equilibrium studies form methylene blue dye by partially hydrolyzed polyacrylamide/cellulose nanocrystal nanocomposite hydrogels, *Chem. Eng. J.*, 251 (2014) 17–24.
- [4] J.A. Gonzalez, M.E. Villanueva, L.L. Piehl, G.J. Copello, Development of a chitin/graphene oxide hybrid composite for the removal of pollutant dyes: adsorption and desorption study, *Chem. Eng. J.*, 280 (2015) 41–48.
- [5] R.B. Wu, K. Zhou, C.Y. Yue, J. Wei, Y. Pan, Recent progress in synthesis, properties and potential applications of SiC nanomaterials, *Prog. Mater. Sci.*, 72 (2015) 1–60.
- [6] M. Bilal, M. Asgher, M. Iqbal, H. Hu, X. Zhang, Chitosan beads immobilized manganese peroxidase catalytic potential for detoxification and decolorization of textile effluent, *Int. J. Bio. Macromol.*, 89 (2016) 181–189.
- [7] Q. Lin, M. Gao, J. Chang, H. Ma, Adsorption properties of crosslinking carboxymethyl cellulose grafting dimethyl-diallyl ammonium chloride for cationic and anionic dyes, *Carbohydr. Polym.*, 151 (2016) 283–294.
- [8] V. Miguez-Pacheco, L.L. Hench, A.R. Boccaccini, Bioactive glasses beyond bone and teeth: emerging applications in contact with soft tissues, *Acta. Biomater.*, 13 (2015) 1–15.
- [9] M.R. Kulkarni, T. Revanth, A. Acharya, P. Bhat, Removal of Crystal Violet dye from aqueous solution using water hyacinth: equilibrium, kinetics and thermodynamics study, *Resour. -Effic. Technol.*, 3 (2017) 71–77.
- [10] P. Simha, A. Yadav, D. Pinjari, A.B. Pandit, On the behaviour, mechanistic modelling and interaction of biochar and crop fertilizers in aqueous solutions, *Resour. -Effic. Technol.*, 2 (2016) 133–142.
- [11] V.M. Vucurovic, R.N. Razmovski, U.D. Miljic, V.S. Puskas, Removal of cationic and anionic azo dyes from aqueous solutions by adsorption on maize stem tissue, *J. Taiwan Inst. Chem. Eng.*, 45 (2014) 1700–1708.
- [12] A.M. Al-Sabagh, M.E. El-Dean, M.A. Hussien, N.A. Farouk, Adsorption kinetics of Zn(II), Cu(II) and Cd(II) Removal by Poly pyrrole/Shells Nanocomposite Adsorbent, *Inter. J. Eng. Sci. Comp.*, 6 (2016) 2226–2233.
- [13] H. Daemi, M. Barikani, M. Barmar, Compatible compositions based on aqueous polyurethane dispersions and sodium alginate, *Carbohydr. Polym.*, 92 (2013) 490–496.

- [14] S. Barreca, S. Orecchio, A. Pace, The effect of montmorillonite clay in alginate gelbeads for polychlorinated biphenyl adsorption: isothermal and kinetic studies, *Appl. Clay Sci.*, 99 (2014) 220–228.
- [15] B. Chen, Z. Yang, G. Ma, D. Kong, W. Xiong, J. Wang, Y. Zhu, Y. Xia, Heteroatom-doped porous carbons with enhanced carbon dioxide uptake and excellent methylene blue adsorption capacities, *Microporous. Mesoporous. Mater.*, 257 (2018) 1–8.
- [16] S.N.A. Rahim, A. Sulaiman, F. Hamzah, K.H.K. Hamid, M.N.M. Rodhi, M. Musa, N.A. Edama, Enzymes encapsulation within calcium alginate-clay beads: characterization and application for cassava slurry saccharification, *Procedia. Eng.*, 68 (2013) 411–417.
- [17] V.K. Gupta, D. Pathania, S. Sharma, S. Agarwal, P. Singh, Remediation and recovery of methyl orange from aqueous solution onto acrylic acid grafted Ficus carica fiber: isotherms, Kinetics and thermodynamics, *J. Mol. Liq.*, 177 (2013) 325–334.
- [18] V.S. Munagapati, D.S. Kim, Equilibrium isotherms, kinetics and thermodynamics studies for Congo red adsorption using calcium alginate beads impregnated with nano-goethite, *Ecotoxic. Environ. Saf.*, 141 (2017) 226–234.
- [19] A.T. Ojedokun, O.S. Bello, Liquid phase adsorption of Congo red dye on functionalized corn cobs, *J. Disp. Sci. Tech.*, 38 (2016) 1285–1294.
- [20] S. Banerjee, M.C. Chattopadhyaya, Adsorption characteristics for the removal of a toxic dye, tartrazine from aqueous solutions by a low cost agricultural by-product, *Arab. J. Chem.*, 10 (2017) 1629–1638.
- [21] K.Z. Elwakeel, A.A. El-Bindary, A.Z. El-Sonbati, A.R. Hawas, Adsorption of toxic acidic dye from aqueous solution onto diethylenetriamine functionalized magnetic glycidyl methacrylate-N,N-methylene bis acrylamide, *RSC. Adv.*, 6 (2016) 3350–3361.
- [22] J. Shu, Z. Wang, Y. Huang, N. Huang, C. Ren, W. Zhang, Adsorption removal of Congo red from aqueous solution by polyhedral Cu₂O nanoparticles: kinetics, isotherms, thermodynamics and mechanism analysis, *J. Alloys. Compd.*, 633 (2015) 338–346.
- [23] G. Vijayakumar, R. Tamilarasan, M. Dharmendirakumar, Adsorption, Kinetic, Equilibrium and Thermodynamic studies on the removal of basic dye Rhodamine-B from aqueous solution by the use of natural adsorbent perlite, *J. Mater. Environ. Sci.*, 3 (2012) 157–170.
- [24] X. Chen, Modeling of experimental adsorption isotherm data, *Information*, 6 (2015) 14–22.
- [25] R. Farouq, N.S. Yousef, Equilibrium and kinetics studies of adsorption of copper (II) ions on natural biosorbent, *Inter. J. Chem. Eng. App.*, 6 (2015) 319–324.
- [26] M.M.F. Silva, M.M. Oliveira, M.C. Avelino, M.G. Fonseca, R.K.S. Almeida, E.C.S. Filho, Adsorption of an industrial anionic dye by modified-KSF-montmorillonite: evaluation of the kinetic, thermodynamic and equilibrium data, *Chem. Eng. J.*, 203 (2012) 259–268.
- [27] S. Agarwal, I. Tyagi, V.K. Gupta, N. Ghasemi, M. Shahivand, M. Ghasemi, Kinetics equilibrium studies and thermodynamics of methylene blue adsorption on Ephedra strobilacea saw dust and modified using phosphoric acid and zinc chloride, *J. Mol. Liq.*, 218 (2016) 208–218.
- [28] A.A. El-Bindary, M.A. Diab, M.A. Hussien, A.Z. El-Sonbati, A.M. Eessa, Adsorption of Acid Red 57 from aqueous solutions onto polyacrylonitrile/activated carbon composite, *Spectrochim. Acta. Part A.*, 124 (2014) 70–77.
- [29] S.A. El-Korashy, K.Z. Elwakeel, A. AbdEl-Hafeiz, Fabrication of bentonite/thiourea-formaldehyde composite material for Pb(II), Mn(VII) and Cr(VI) sorption: a combined basic study and industrial application, *J. Cleaner. Prod.*, 137 (2016) 40–50.
- [30] E.U. Deveci, N. Dizge, H. C. Yatmaz, B. Tansel, Degradation of recalcitrant textile dyes by coupling fungal and photocatalytic membrane reactors. *CLEAN–Soil. Air. Water.*, 44 (2016) 1345–1351.
- [31] L. Li, H. Wang, Z. Zhang, X. Chen, Q. Li, Facile synthesis of bioglass nanospheres for the adsorption of cationic and anionic dyes from aqueous solution, *J. Dispersion. Sci. Technol.*, 38 (2017) 1711–1718.
- [32] V.S. Munagapati, D.S. Kim, Equilibrium isotherms, kinetics, and thermodynamics studies for congo red adsorption using calcium alginate beads impregnated with nano-goethite, *Ecotoxicol. Environ. Saf.*, 141 (2017) 226–234.
- [33] R. Lafi, K. Charradi, M.A. Djebbi, A.B.H. Amara, A. Hafiane, Adsorption study of Congo red dye from aqueous solution to Mg–Al-layered double hydroxide, *Adv. Powder. Technol.*, 27 (2016) 232–237.
- [34] Y. Shang, J. Zhang, X. Wang, R. Zhang, W. Xiao, S. Zhang, R. Han, Use of polyethyleneimine-modified wheat straw for adsorption of Congo red from solution in batch mode, *Desal. Wat. Treat.*, 57 (2015) 8872–8883.
- [35] R. Zhang, J. Zhang, X. Zhang, C. Dou, R. Han, Adsorption of Congo red from aqueous solutions using cationic surfactant modified wheat straw in batch mode: kinetic and equilibrium study, *J. Taiwan. Inst. Chem. Eng.*, 45 (2014) 2578–2583.
- [36] R. Fabryanty, C. Valencia, F.E. Soetaredjo, J.N. Putro, S.P. Santoso, A. Kurniawan, Y.H. Ju, S. Ismadji, Removal of crystal violet dye by adsorption using bentonite – alginate composite, *J. Environ. Chem. Eng.*, 5 (2017) 5677–5687.
- [37] L. Aref, A.H. Navarchian, D. Dadkhah, Adsorption of crystal violet dye from aqueous solution by poly(acrylamide-co-maleic acid)/montmorillonite nanocomposite, *J. Ploym. Environ.*, 25 (2017) 628–639.
- [38] T.H. Nazifa, N. Habba, Salmiati, A. Aris, T. Hadibarata, Adsorption of Procion Red MX-5B and Crystal Violet Dyes from aqueous solution onto corncob activated carbon, *J. Chin. Chem. Soc.*, 65 (2018) 259–270.

Supplementary material

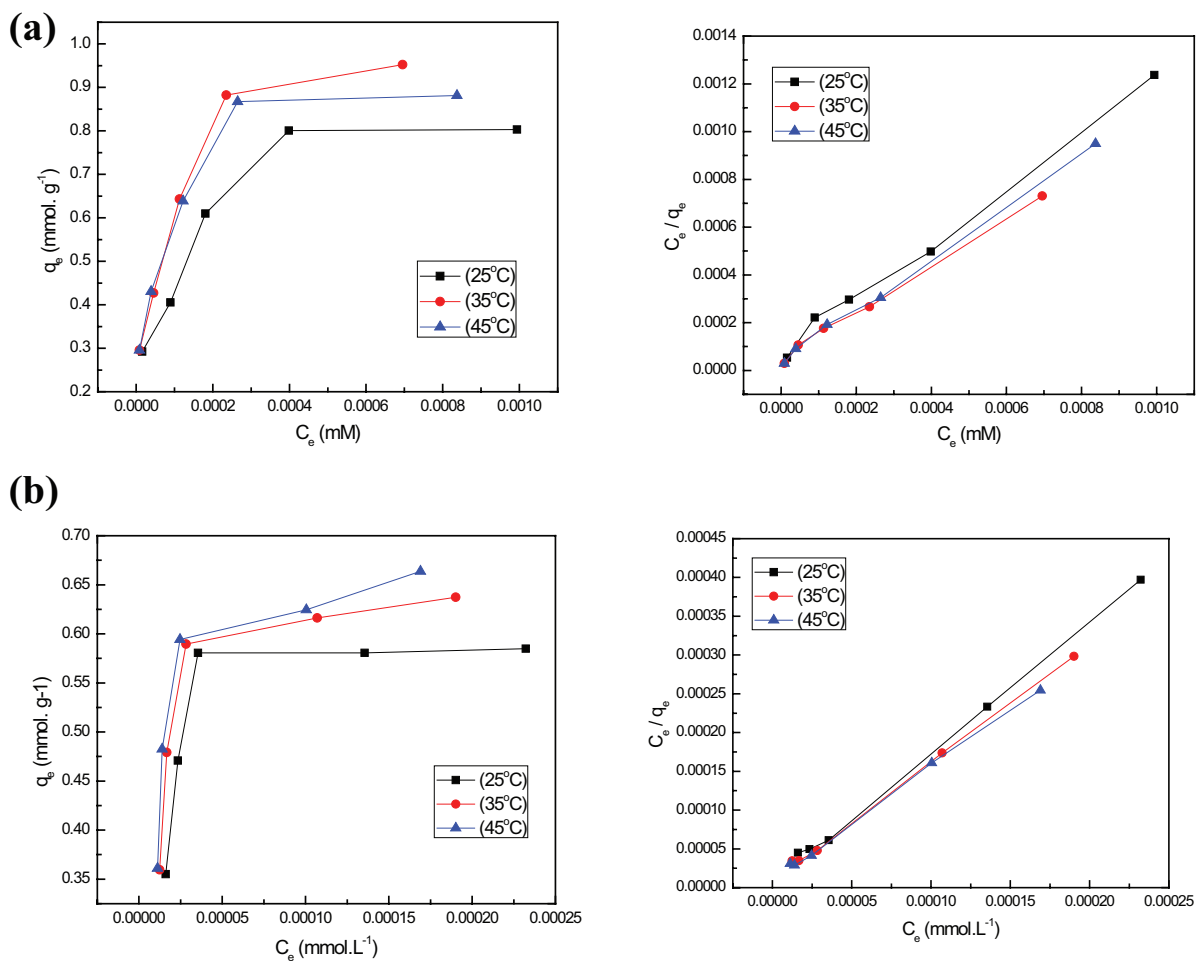


Fig. S1. Effect of initial dye concentration (a) ($6, 9, 14, 20, 26 \times 10^{-4}$ mmol.L⁻¹) of CR and (b) ($3, 4, 5, 6, 7 \times 10^{-4}$ mmol.L⁻¹) of CV using (0.05 and 0.02 g) of (TUFA) respectively at different temperatures (25°C, 35°C, 45°C).

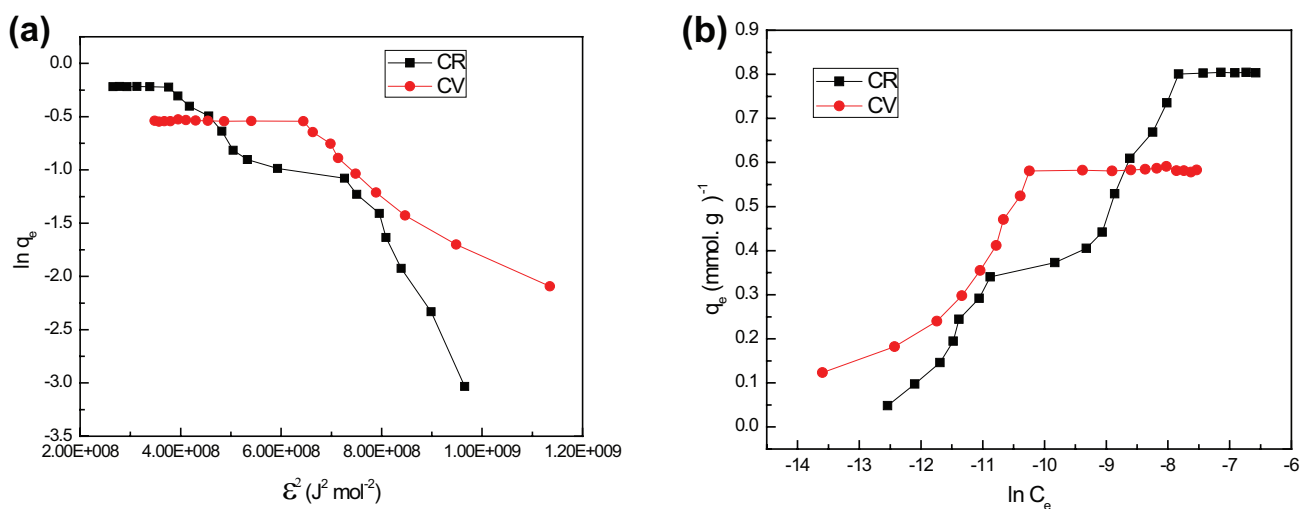


Fig. S2. Adsorption isotherm (a) Dubinin–Radushkevich, (b) Temkin model for ($1 \times 10^{-4} - 3 \times 10^{-3}$ mmol.L⁻¹) of CR and ($1 \times 10^{-4} - 1 \times 10^{-3}$ mmol.L⁻¹) of CV on (0.05 and 0.02 g) of (TUFA) respectively at 25°C \pm 1°C.

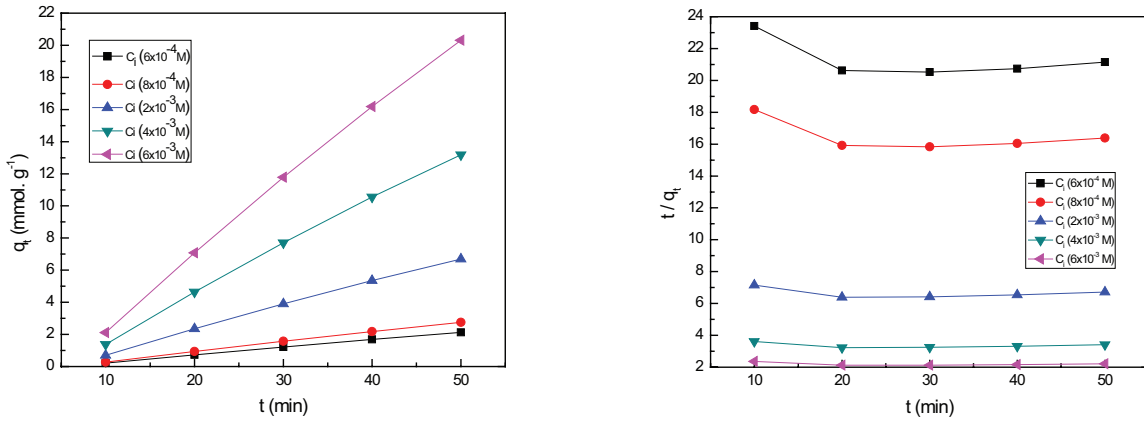


Fig. S3. Effect of contact time for (6, 8, 20, 40, 60 × 10⁻⁴ mmol.L⁻¹) of CR on (0.05 g) of (TUFA) at different initial dye concentrations.

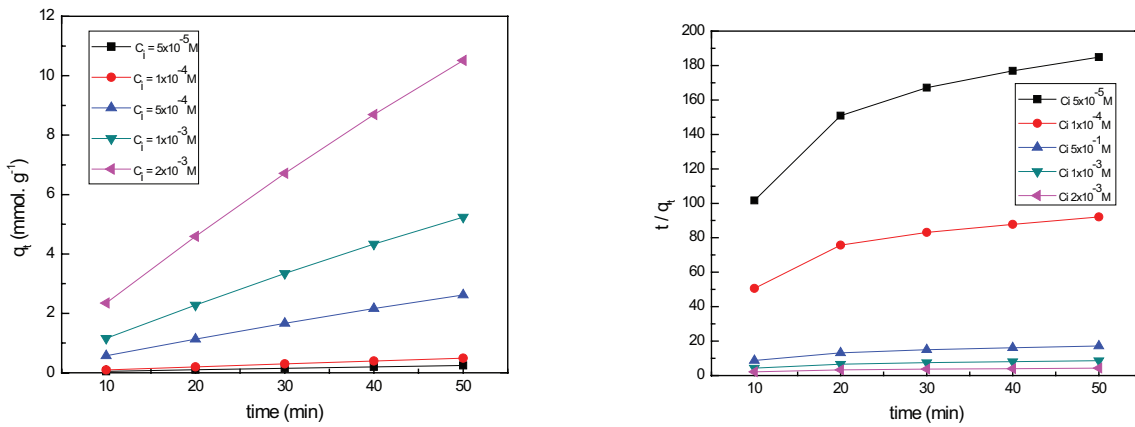


Fig. S4. Effect of contact time for (5, 10, 50, 100, 200 × 10⁻⁴ mmol.L⁻¹) of CV on (0.02 g) of (TUFA) at different initial dye concentrations.

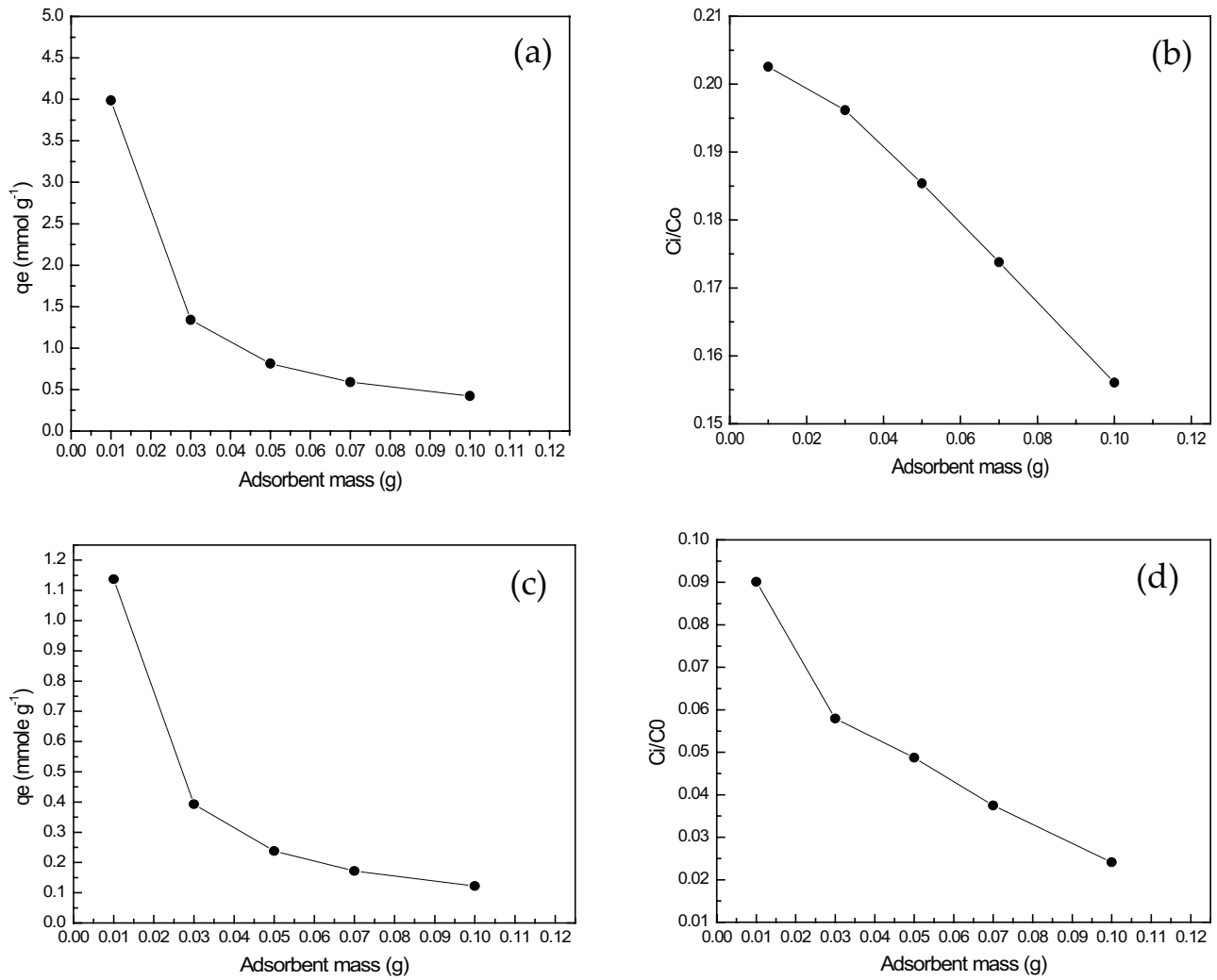


Fig. S5. Effect of sorbent dose for (0.01 – 0.1 g) (TUFA) (a, b) for CR and (c, d) for CV on adsorption.

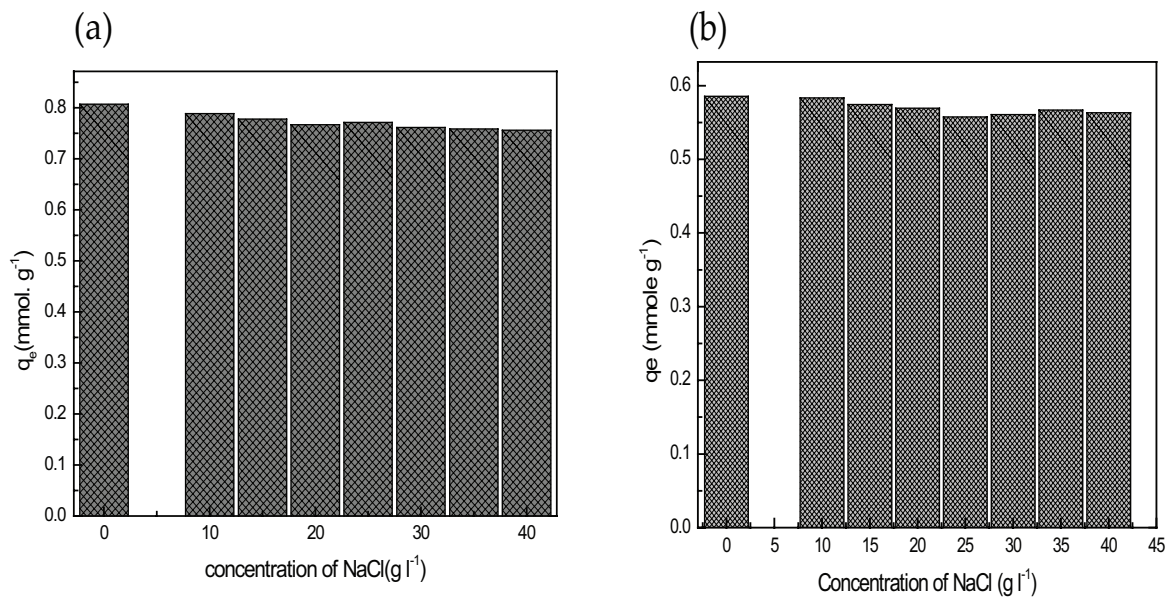


Fig. S6. Effect of ionic strength (a) for CR and (b) for CV on (0.05 and 0.02 g) of (TUFA) respectively at $25^\circ C \pm 1^\circ C$ (addition of NaCl).